Research Article
doi.org/10.1002/elsa.202100100

Chemistry Europe
European Chemical Societies Publishing

Received: 25 May 2021
Revised: 14 August 2021
Accepted: 10 September 2021

Enhancing the catalytic current response of H_2 oxidation gas diffusion bioelectrodes using an optimized viologen-based redox polymer and [NiFe] hydrogenase

Anna Lielpetere[1] | **Jana M. Becker**[1] | **Julian Szczesny**[1] | **Felipe Conzuelo**[1] | **Adrian Ruff**[1] | **James Birrell**[2] | **Wolfgang Lubitz**[2] | **Wolfgang Schuhmann**[1]

[1] Faculty of Chemistry and Biochemistry, Analytical Chemistry – Center for Electrochemical Sciences (CES), Ruhr University Bochum, Bochum, Germany

[2] Max Planck Institute for Chemical Energy Conversion, Mülheim an der Ruhr, Germany

Correspondence
Wolfgang Schuhmann, Faculty of Chemistry and Biochemistry, Analytical Chemistry – Center for Electrochemical Sciences (CES), Ruhr University Bochum, Universitätsstr. 150, D-44780 Bochum, Germany.
Email: wolfgang.schuhmann@rub.de

Funding information
H2020 Marie Skłodowska-Curie Actions MSCA-ITN "ImplantsSens" [813006]; Deutsche Forschungsgemeinschaft in the framework of the SPP 3561927 "Iron–Sulfur for Life", Grant/Award Number: BI 2198/1-1

Abstract

Using viologen-based redox polymers to wire a variety of different hydrogenases to electrodes and gas diffusion electrodes is the basis to mitigate high potential deactivation of the enzyme, deactivation by molecular O_2, as well as for high-current density H_2 oxidation bioanodes. To overcome electron transfer limitations by electron hopping within the viologen-modified polymer film, a new redox polymer was designed with the highest possible viologen content together with monomers bearing crosslinking units. In combination with an immobilization sequence consisting of oxidative grafting of amino functions, covalent attachment of polymer units to these functionalities, and crosslinking of the polymer layers, an unprecedently fast electron transfer became possible. This enabled a very high current density normalized by the amount of the [NiFe] hydrogenase embedded within a viologen polymer on gas diffusion electrodes.

KEYWORDS
bioanode, gas diffusion electrode, hydrogen oxidation, hydrogenase, redox polymer

1 | INTRODUCTION

Nature evolved highly efficient biocatalysts for the oxidation and formation of H_2 with active centers consisting solely of earth abundant metals like Ni and Fe[1] and a catalytic performance similar to that of Pt.[2–7] Hydrogenases have been employed as hydrogen oxidation catalysts at the anode of H_2/O_2 biofuel cells[2–4,7] while multicopper oxidases like bilirubin oxidase or laccase have been used as O_2 reduction catalysts at the cathode.[8] The use of hydrogenases in large-scale applications is limited by their generally high sensitivity towards O_2 and their deactivation at high electrochemical potentials.[2–4,9–11] Enzyme engineering does not offer a satisfying solution to this challenge as frequently increased intrinsic stability of an enzyme leads to a decreased catalytic performance.[1,12]

The incorporation of hydrogenases into low-potential viologen-modified polymer matrices offers immobilization, electrical connection, as well as protection against O_2 and high-potential deactivation.[13–19] On the one hand, redox polymers provide a Nernst buffer which lowers the local potential at the enzyme, especially under turnover conditions, and is thereby protecting the enzyme by preventing its oxidation to an inactive state. On the other

Research Article
doi.org/10.1002/elsa.202100100
Chemistry Europe
European Chemical Societies Publishing

hand, the viologen radical cations are able to reduce incoming O_2 with electrons generated during the catalytic H_2 oxidation, protecting the enzyme from deactivation or even destruction through exposure to O_2.[20]

To avoid limitations in performance by slow mass transport of the gaseous substrate, the use of gas diffusion electrodes (GDEs) has been shown to be essential.[21–27] GDEs typically consist of a porous carbon-based material that guarantees gas permeability in combination with a hydrophobic layer (e.g., polytetrafluoroethylene) to prevent leakage of aqueous electrolytes.[28] A triple-phase boundary is established between the liquid electrolyte, gaseous substrate, and solid electrode/catalyst material. Diffusion of the substrate takes place by rapid dissolution from the gas phase into a thin electrolyte layer that is formed around the catalyst due to a large concentration gradient between the gaseous and liquid phases. The local substrate flux towards the catalyst sites is substantially increased, which is the basis for the observed enhanced current densities at corresponding electrodes.[25,29]

In our previous work, we combined the benefits of redox polymers, namely protection of the enzyme and high catalyst loading, with the concept of gas diffusion electrodes to fabricate high performance H_2 oxidation bioanodes using various hydrogenases as biocatalysts.[17,18,30] Surprisingly, the catalytic current response of these electrodes did not scale with the intrinsic activity of the employed hydrogenase.[17] Since H_2 mass transport limitation could be ruled out when using GDEs, the limited current densities achieved, especially in the case of the most active [FeFe] hydrogenase,[18] may be attributed to insufficient electron transfer kinetics within the redox polymer film.[17] To prevent direct electron transfer with the immobilized hydrogenase, which would lead to undesired enzyme inactivation, an initial coating of the GDE surface with a layer of only the redox polymer without any enzyme was used as an adhesion layer between the electrode surface and the catalytically active layer comprising a mixture of redox polymer and hydrogenase. To improve adhesion of the first polymer layer on the hydrophobic GDE surface, the redox polymer employed for the adhesion layer was designed to possess on the one hand, a lower content of the positively charged viologen moieties and on the other hand a higher number of monomer units with hydrophobic side chains. We assume that by this the probability of the collision between adjacent viologen units within the redox polymer layer is insufficient to allow charge transfer at the rate necessary for the most active hydrogenase at high enzyme loading and unlimited H_2 supply within the GDE.[17,18,30]

We hypothesize that by the design of a redox polymer with higher viologen loading compared to 71% and 65%,[16] but still high stability on the hydrophobic GDE surface the electron transfer rate within the polymer can be enhanced, thus allowing even the most active hydrogenases to turn over with their intrinsic rate. We demonstrate that the design of such a polymer together with an immobilization strategy relying solely on covalent crosslinking is the basis for hydrogenase-modified GDEs with high H_2 oxidation currents and stability.

2 | RESULTS AND DISCUSSION

We designed the redox copolymer (poly(3-azido-propyl methacrylate-*co*-glycidyl methacrylate)-1-(hex-5-yn-1-yl)-1′-methyl-[4,4′bipyridinium] (*co*P(N_3MA^{85}-GMA^{15})-vio) with a particularly high viologen content of 85 mol% (Figure 1). Only two monomers were used, namely one bearing an azido-group for later binding of the viologen unit by means of a Cu-catalysed click reaction and a second with an epoxide unit for covalent attachment to the modified electrode surface and reaction with bifunctional crosslinkers. The surface of the carbon cloth GDE is functionalized by means of oxidative electrografting of half-protected diamines,[32] which additionally improves the compatibility between the hydrophobic electrode material and the rather hydrophilic redox hydrogel (Figure 2a). The newly synthesized polymer exhibits a redox potential of -296 mV versus standard hydrogen electrode (SHE) (Figure S1), which is 128 mV more positive than the potential of the $H_2/2H^+$ couple at pH 7 and 298.15 K (−414 mV vs. SHE). This potential difference is sufficiently large to invoke a high driving force for H_2 oxidation, but it is still low enough to guarantee a large open-circuit voltage in a corresponding biofuel cell.[33] The optimization of the polymer loading on the electrode in a two-layer approach (Figure 2b), similar to the ones described in our previous work,[16–18] yielded highly stable GDEs with immobilized [NiFe] hydrogenase from *Desulfovibrio vulgaris* Miyazaki F (*Dv*MF).

The high hydrophilicity of the redox polymer *co*P(N_3MA^{85}-GMA^{15})-vio is obviously incompatible with the initially highly hydrophobic GDE surface. Cyclic voltammograms of a redox polymer-modified GDE recorded in Ar-saturated 0.1 M phosphate buffer (pH 7.4) showed diminishing redox signals after only a few potential cycles, most likely due to dissolution of the hydrophilic polymer into the electrolyte (Figure 3a). We decided to use oxidative electrografting of ethylenediamine on the GDE surface prior to modification with *co*P(N_3MA^{85}-GMA^{15})-vio.

On one hand, the surface modification strongly increased the hydrophilicity of the GDE which in turn enhances the compatibility between the properties of the electrode surface and the redox polymer. On the

Research Article
doi.org/10.1002/elsa.202100100
Chemistry Europe
European Chemical Societies Publishing

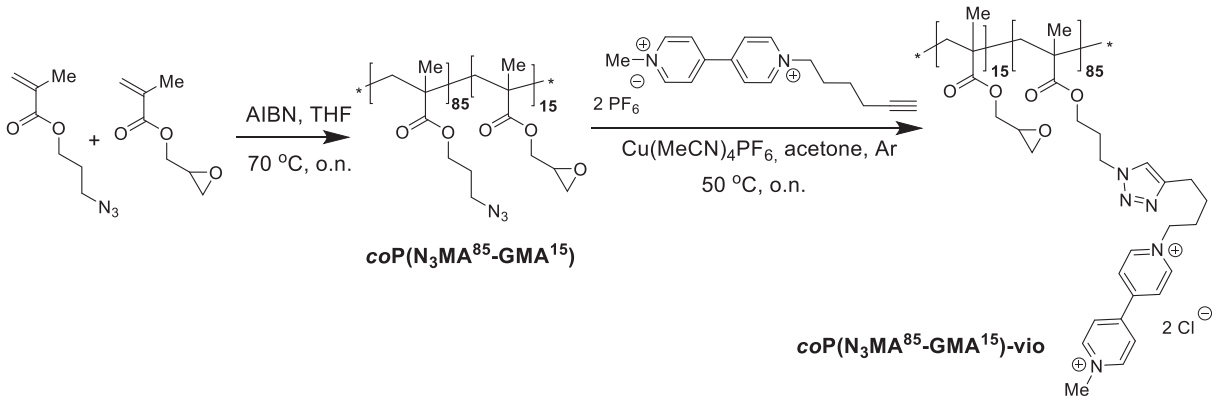

FIGURE 1 Scheme of the synthetic pathway towards the high viologen content redox polymer *co*P(N_3MA^{85}-GMA^{15})-vio (for the detailed synthesis see experimental section)

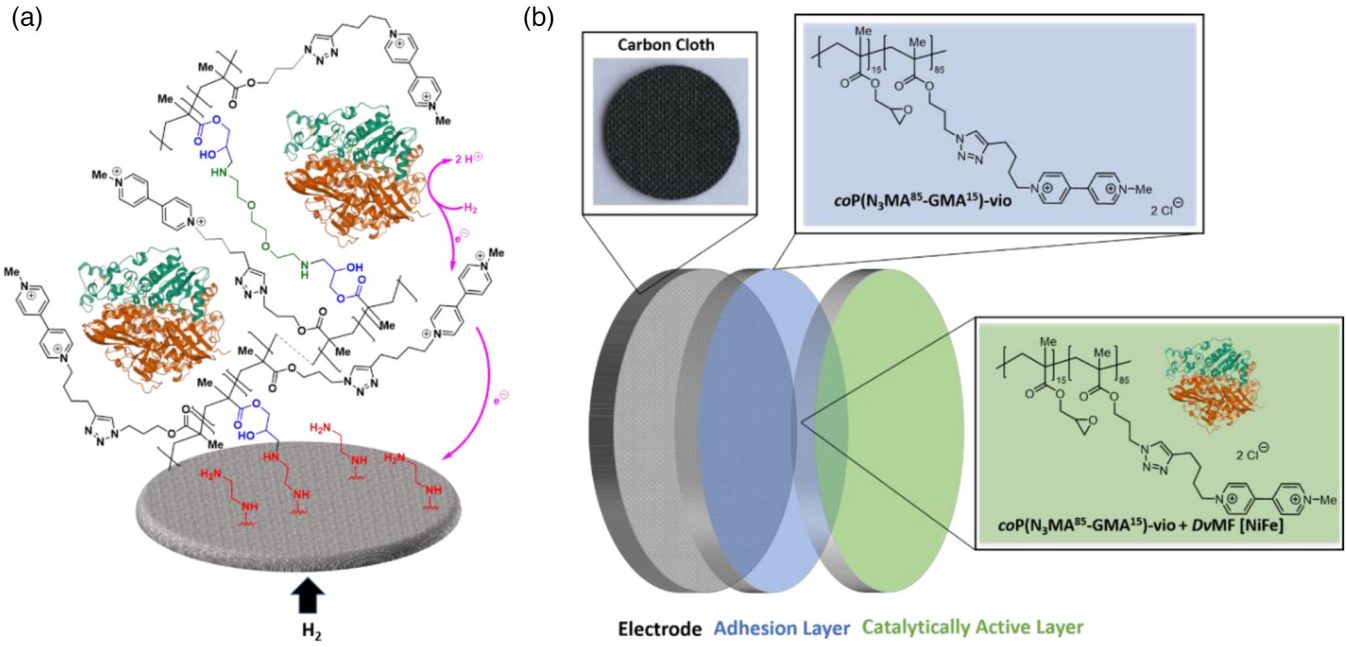

FIGURE 2 (a) Schematic illustration of a carbon cloth-based gas diffusion electrode modified with [NiFe] hydrogenase from *Desulfovibrio vulgaris* Miyazaki F (*Dv*MF) and *co*P(N_3MA^{85}-GMA^{15})-vio covalently bound to the electrografted electrode surface via an ethylenediamine linker and crosslinked with 2,2′-(ethylenedioxy)bis(ethylamine) (not drawn to scale). (b) Schematic illustration of the two-layer configuration used for electrode modification

other hand, the surface-tethered amino-functionalities can be used as anchor sites for covalent attachment of the polymer chains via an epoxide ring-opening reaction as schematically shown in Figure 2a, and this leads to improved stability of the hydrogel film (Figure 3b).

Additional reaction with the bifunctional crosslinker 2,2′-(ethylenedioxy)bis(ethylamine) creates a highly stable three-dimensional polymer network on the GDE in which the polymer chains are covalently interconnected as well as linked to the electrode surface and reacted with the lysine residues at the surface of the integrated enzymes (Figure 3c). The catalytic current response of redox polymer-based bioelectrodes is considered to be dependent on the polymer film thickness, which determines the number of electron-hopping steps for the charge transfer, the necessary counter ion movement, and local pH changes as a consequence of the enzyme-catalyzed reaction. Hence, optimization of the polymer loading is essential to obtain a maximal enzyme loading with the goal of maximum H_2 oxidation currents while not compromising the charge transfer as well as substrate and product diffusion. Optimization was carried out sequentially by keeping initially a constant hydrogenase loading of 110 µg. The polymer amount used for the adhesion layer was varied, while

Research Article
doi.org/10.1002/elsa.202100100
Chemistry Europe
European Chemical Societies Publishing

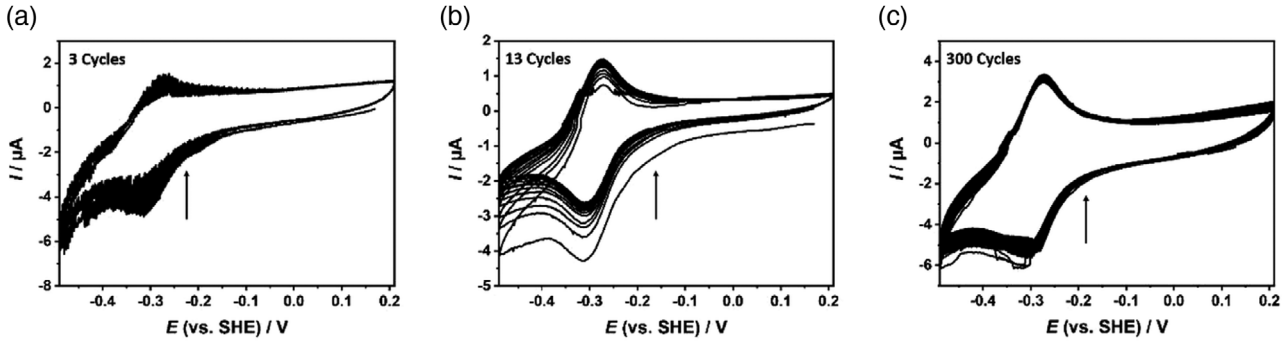

FIGURE 3 Cyclic voltammograms of carbon cloth gas diffusion electrodes modified with (a) *co*P(N_3MA^{85}-GMA^{15})-vio (no crosslinker, no electrografting, 3 cycles), (b) *co*P(N_3MA^{85}-GMA^{15})-vio covalently bound to the electrografted electrode surface via an ethylenediamine linker (no crosslinker, 13 cycles) and (c) *co*P(N_3MA^{85}-GMA^{15})-vio bound to the electrografted electrode surface via an ethylenediamine linker and crosslinked with 2,2′-(ethylenedioxy)bis(ethylamine) (300 cycles). Measurements were conducted in Ar saturated 0.1 M phosphate buffer pH 7.4 with a scan rate of 10 mV/s

the relative amount of redox polymer and hydrogenase in the active layer remained constant. Chronoamperometric measurements were performed at a fixed potential of +160 mV vs. SHE to minimize the influence of capacitive currents which cannot be neglected in potentiodynamic measurements at high surface area electrodes. Low catalytic currents at a low polymer amount in the adhesion layer are most likely attributed to direct electron transfer of a part of the enzyme molecules with the electrode leading to high-potential deactivation of the enzyme. In contrast, thick adhesion layers decrease the electron transfer rate within the film and increase substrate and product diffusion pathways, which together limit the catalytic current. The optimal polymer amount in the adhesion layer was found to be 50 µg (Figure 4a, Table S1). Subsequently, the polymer loading in the active layer was varied while the polymer amount in the adhesion layer was kept at 50 µg. Following a bell-shaped function, a maximum catalytic current of 496 ± 135 µA was obtained with a polymer loading of 100 µg (polymer/enzyme ratio ≈ 1:1.1 (w/w)) in the active layer (Figure 4B, Table S2).

We assume that small currents at low polymer loadings in the active layer are the result of inefficient enzyme wiring and slow electron transfer kinetics, while low currents at high polymer loadings can be explained by limitations in the substrate and product diffusion as well as the charge transfer rate within the film.

Finally, we compared the performance of the optimized GDE based on the specifically designed high-viologen loading (85 mol%) polymer *co*P(N_3MA^{85}-GMA^{15})-vio with the results that were obtained with a viologen-modified polymer with a viologen content of only 71 mol% and the same hydrogenase as evaluated under the same conditions as previously.[16]

The cyclic voltammograms (CVs) show the productive wiring of the polymer-integrated hydrogenase in presence of H_2 in both cases (Figure 5a, solid red and dashed blue curves). High potential deactivation or deactivation of the enzyme by O_2 was not observed (Figure S5). Most importantly, the measured plateau current for H_2 oxidation for the optimized GDE based on the newly designed polymer with increased viologen content reached an unprecedented value of 794 µA which is approximately twice as high as the ones obtained with the lower viologen-content polymer (389 µA). The higher electrochemical response of $P_{vio71\%}$ under non-turnover conditions compared to $P_{vio85\%}$ is attributed to a larger polymer loading and a favored interaction within the more hydrophobic polymer backbone due to the smaller number of positively charged viologen units and 20 % of the highly hydrophobic butyl acrylate co-monomer. Under turnover conditions, close interaction between the enzyme and the redox relay, and fast electron transport within the film are required, which is achieved by the more hydrophilic $P_{vio85\%}$ polymer which should also facilitate film swelling and counter ion movement. Moreover, the higher number of positive charges in $P_{vio85\%}$ favor a strong interaction with the negatively charged part of the hydrogenase around the terminal FeS cluster ensuring efficient electron extraction from the enzyme during turnover. The somewhat distorted shape of the CVs of the electrode modified with $P_{vio85\%}$ in the reductive region (Figure 5a, solid black line) is associated with the catalytic formation of H_2 by the biocatalyst embedded within the redox polymer matrix as can be rationalized from the CVs performed in the absence of H_2 at an electrode modified with $P_{vio85\%}$ and inactivated [NiFe] hydrogenase compared to those obtained for an electrode modified with $P_{vio85\%}$ and active [NiFe] (Figure S9).

The stability of the optimized H_2 oxidation GDE was evaluated under continuous operation under turnover conditions (Figure 5b). The decrease in the catalytic current response is associated with loss of the polymer film as

Research Article
doi.org/10.1002/elsa.202100100
Chemistry Europe
European Chemical Societies Publishing

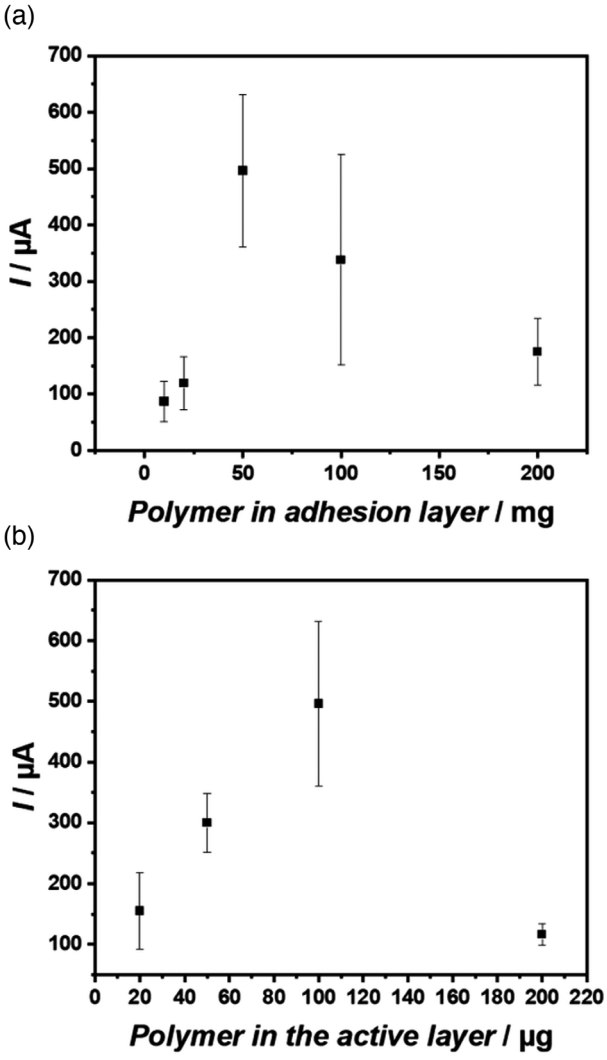

FIGURE 4 Catalytic currents obtained from three ethylenediamine electrografted gas diffusion electrode (GDEs) modified with a *co*P(N_3MA^{85}-GMA^{15})-vio adhesion layer, a *co*P(N_3MA^{85}-GMA^{15})-vio/*Dv*MF [NiFe] hydrogenase, and 2,2′-(ethylenedioxy)bis(ethylamine) as crosslinker (13 µg). Currents from chronoamperometric measurements in 0.1 M phosphate buffer pH 7.4 at an applied potential of 0.16 V versus standard hydrogen electrode (SHE) after t = 900 s. (a) Different loadings of *co*P(N_3MA^{85}-GMA^{15})-vio in the adhesion layer with constant polymer and enzyme loading in the active layer: Polymer loading in the active layer = 100 µg. Enzyme loading = 110 µg. (b) Different loadings of *co*P(N_3MA^{85}-GMA^{15})-vio in the active layer with constant enzyme loading and constant polymer loading in the adhesion layer. Enzyme loading = 110 µg. Polymer loading in the adhesion layer = 50 µg. Error bars indicate the standard deviation

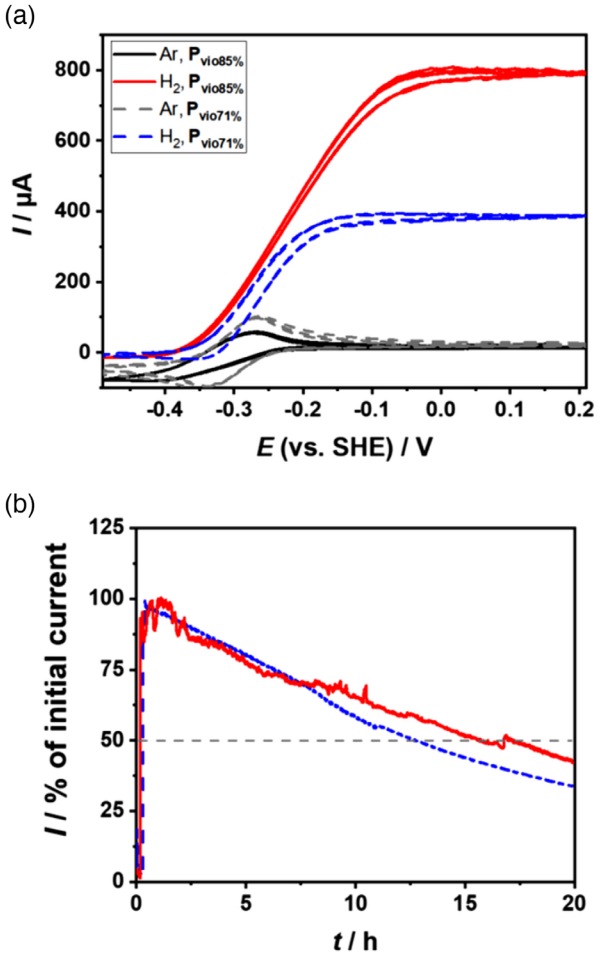

FIGURE 5 (a) Cyclic voltammograms of an ethylenediamine-electrografted gas diffusion electrode (GDE) modified in a two-layer configuration with the high-viologen loading redox polymer *co*P(N_3MA^{85}-GMA^{15})-vio, 2,2′-(ethylenedioxy)bis(ethylamine) as crosslinker and *Dv*MF [NiFe] hydrogenase in 0.1 M phosphate buffer (pH 7.4) under turnover (red solid curve) and non-turnover (black solid curve) conditions. v = 10 mV/s. Measurements conducted with an electrode based on a polymer with a lower viologen loading and the same biocatalyst under the same conditions are shown as comparison[16] (dashed grey curve, non-turnover and dashed blue curve, turnover). Note that the polymer loading for the electrode modified with $P_{vio85\%}$ is lower (150 µg) compared with the electrode modified with $P_{vio71\%}$ (230 µg). (b) Chronoamperometry of an ethylenediamine-electrografted GDE modified in a two-layer configuration with the high-viologen loading redox polymer *co*P(N_3MA^{85}-GMA^{15})-vio, 2,2′-(ethylenedioxy)bis(ethylamine) as a crosslinker and *Dv*MF [NiFe] hydrogenase under turnover conditions in 0.1 M phosphate buffer (pH 7.4). E_{app} = 160 mV versus standard hydrogen electrode (SHE)

a decrease in the current response from the redox mediator can be observed in cyclic voltammograms recorded after the long-term measurement (Figure S10). A 50% loss of the initial current was reached after 16 h which reflects a 50% increase in longevity compared to H_2 oxidation GDEs, in which the polymer film adhered solely by hydrophobic interaction at the electrode surface, and the immobilization was performed without further crosslinking.[16]

To ultimately confirm that the newly designed redox polymer with high-viologen content is able to mitigate possible electron transfer limitations within the polymer

Research Article
doi.org/10.1002/elsa.202100100
Chemistry Europe
European Chemical Societies Publishing

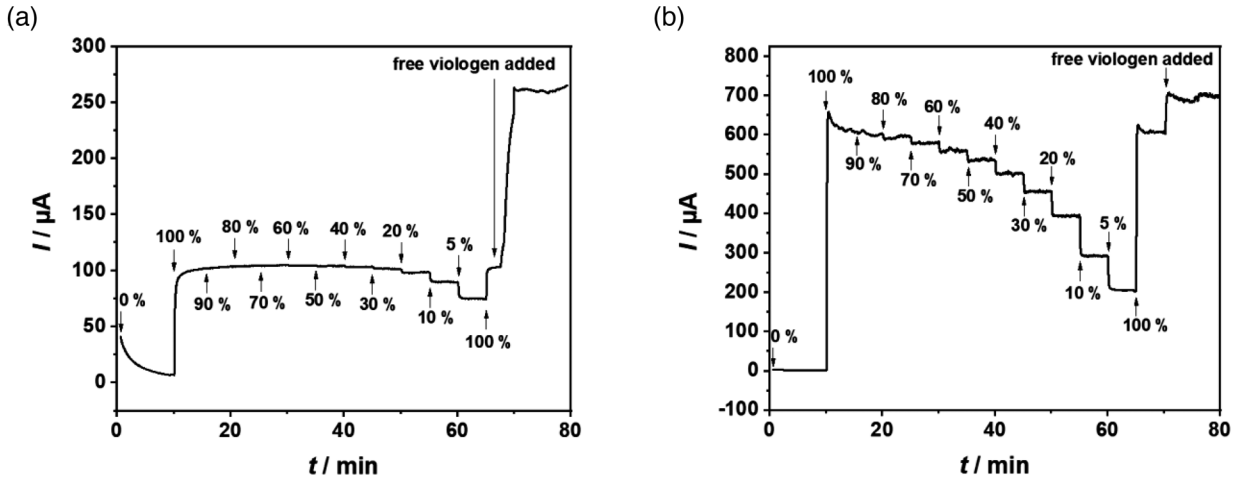

FIGURE 6 Influence of the partial pressure of H_2 and addition of freely diffusing dimethylviologen: Chronoamperometric measurement in 0.1 M phosphate buffer pH 7.4 with an applied potential of 0.16 V versus standard hydrogen electrode (SHE) of (a) Carbon-cloth gas diffusion electrode (GDE) modified with P(GMA^{65}-BA^{32}-PEGMA^{9})-vio adhesion layer (loading 150 µg), a P(N$_3$MA^{71}-BA^{20}-GMA^{9})-vio (loading 89 µg)/*Dv*MF [NiFe] hydrogenase (loading 110 µg) (prepared according to a previously published procedure[16]) and (b) Carbon-cloth GDE modified with a *co*P(N$_3$MA^{85}-GMA^{15})-vio adhesion layer (loading 50 µg), a *co*P(N$_3$MA^{85}-GMA^{15})-vio (100 µg)/*Dv*MF [NiFe] hydrogenase (loading 110 µg) and 2,2′-(ethylenedioxy)bis(ethylamine) as crosslinker (13 µg). Gas mixtures with varying amounts of H_2 (amount of H_2 shown in the graphs) and Ar provided in the gas feed of the GDE. Freely diffusing 1,1′-dimethyl-4,4′-bipyridinium diiodide was added in excess at $t = 68$ min (a) and $t = 70$ min (b)

film, we performed comparative experiments using the two-layer hydrophobic polymer system as used in our previous work,[16] namely a carbon-cloth GDE modified with P(GMA^{65}-BA^{32}-PEGMA^{9})-vio as adhesion layer (loading 150 µg) (Figures 6a), and an active layer containing P(N$_3$MA^{71}-BA^{20}-GMA^{9})-vio (loading 89 µg)/*Dv*MF [NiFe] hydrogenase (loading 110 µg), and the optimized GDE as described above (Figures 6b). First, the H_2 concentration in the gas feed behind the GDEs was stepwise reduced by dilution with Ar to evaluate the turning point at which the availability of H_2 becomes limiting for the measured H_2 oxidation. The non-optimized electrode design shows a comparatively low H_2 oxidation current at 100% H_2 in the gas feed, which remained nearly unchanged until about 30% H_2. After changing back to 100% H_2, addition of freely diffusing viologen leads to a significant increase of 159 µA (154%) in the catalytic current which is indicative of the inability of this electrode configuration to assure sufficiently fast charge transfer between the immobilized hydrogenase and the electrode via the polymer-attached viologen units (Figure 6a). In contrast, in the case of the newly developed and optimized electrode architecture a much higher H_2 oxidation current is obtained at 100% H_2 in the gas feed behind the GDE. Moreover, this current immediately decreases if the H_2 concentration in the gas feed is lowered suggesting substrate limitation.

However, most importantly, upon the addition of free-diffusing viologen, only a moderate increase of 85 µA (14%) in the catalytic current can be observed (Figure 6b). These results clearly indicate that slow electron transfer kinetics limit the performance of the system with low viologen content in the polymer. By designing a new high-viologen loaded polymer and establishing a secure immobilization strategy exclusively based on covalent bonds, we have shown a significantly enhanced performance of the H_2 oxidation GDE mitigating the limiting electron transfer rate within the redox polymer (Table S3).

3 | CONCLUSION

The design of a high-viologen loading redox polymer *co*P(N$_3$MA^{85}-GMA^{15})-vio together with an all-covalent immobilization strategy leads to improved electron transfer rates which in return allow for larger currents when *Dv*MF [NiFe] hydrogenase is employed as H_2 oxidation biocatalyst. Comparing with results obtained with a redox polymer containing fewer viologen moieties the H_2 oxidation current was doubled by only increasing the viologen content by 14%. The addition of a freely diffusing mediator led to only a minor increase in the catalytic current confirming that the electron transfer through the polymer film was no longer limiting the electrode performance. Further improvements in the bioelectrode stability could be achieved by the implementation of more efficient redox polymers that enhance substrate and electron transfer or offer more effective cross-linking strategies. Potential strategies could involve the formation of highly

Research Article
doi.org/10.1002/elsa.202100100

stable amide bonds in the crosslinking process, the use of less hydrophobic electrode materials to improve the interaction between electrode and polymer, and the design of advanced electrode architectures using stabilizing capping layers.

4 | EXPERIMENTAL SECTION

4.1 | Chemicals

All chemicals were purchased from Sigma-Aldrich, Alfa Aesar, Acros Organics, VWR, Supelco, TCI, and Roth and used as received unless otherwise noted. Dry solvents were purchased from Acros Organics (extra dry, stored over molecular sieves, AcroSeal bottles). Deuterated solvents were from Deutero or Eurisotop and were stored at 4°C, dimethyl sulfoxide (DMSO)-d_6 was stored at room temperature. Commercially available monomers were passed through a column containing the corresponding inhibitor remover (Sigma-Aldrich) and stored at –20°C. $[Cu(MeCN)_4]PF_6$ was stored in a desiccator at room temperature. All reactions and manipulations were conducted using the standard Schlenk technique under Ar atmosphere. All aqueous solutions were prepared using water purified and deionized with a Milli-Q system. Gases were purchased from Air Liquide and were of 4.0 quality or higher.

4.2 | Enzymes

[NiFe] hydrogenase from *Desulfovibrio vulgaris* Miyazaki F was isolated and purified[31] and stored in MES buffer (pH 6.8) at −80 °C with a concentration of 882 µM.

4.3 | Spectroscopy

^{1}H-NMR spectra were recorded with a DPX200 spectrometer from Bruker. The residual solvent peak was used as an internal standard for the determination of chemical shifts. Ultraviolet-visible measurements were performed with a Cary 60 spectrophotometer from Agilent Technologies in quartz cuvettes with an optical path length of 1 cm.

4.4 | Redox polymer synthesis

Synthesis of the high viologen loading redox polymer coP(N_3MA^{85}-GMA^{15})-vio: Recrystallisation of the radical initiator 2,2-azobis(2-methylpropionitrile) (AIBN) and synthesis of 3-azido-propyl methacrylate (N_3MA) and (1-(5-hexyn-1-yl)-1′-methyl-4,4′-bipyridinium dihexafluorophosphate) was performed according to previously published procedures.[15]

Synthesis of the polymer backbone *co*P(N_3MA^{85}-GMA^{15}): 3-azido-propyl methacrylate (N_3MA, 1.0 g, 5.9 mmol, 95 mol%) and glycidyl methacrylate (GMA, inhibitor-free, 40 µl, 0.3 mmol, 5 mol%) were added to a Schlenk tube (dried by 3 Ar-vacuum cycles), dissolved in tetrahydrofuran (10 ml), and the solution was deaerated by flushing with Ar. Then, azobisisobutyronitrile (7 mg) was added, and the mixture was heated at 70°C overnight. After cooling to room temperature, the polymer was precipitated with *n*-pentane (60 ml), forming a yellow translucent gel which was separated by centrifugation (4000 rpm, 20 min), re-dissolved in tetrahydrofuran (~8 ml), then precipitated with diethyl ether (~35 ml) and separated by centrifugation (4000 rpm, 30 min). The product was dried in vacuum at room temperature overnight. The white solid was dissolved in acetone (concentration 70 mg/ml) and stored in the dark at 4°C. The final composition of the polymer was determined by the ^{1}H-NMR integral ratio: 85% N_3MA, 15% GMA. The epoxide signal at 3.2 ppm was used for the determination of the ratio due to the smallest overlap with other signals. ^{1}H-NMR (200 MHz, acetone-d_6) δ/ppm: 4.3 (multiplet, -CH_2O- of GMA), 4.1 (broad, -CH_2O- of N_3MA), 3.8 (multiplet, epoxide), 3.6 (triplet, -CH_2-N_3, J = 6.4 Hz), 3.2 (broad, epoxide), 2.8 & 2.6 (2 multiplets partially overlapping with water, epoxide), 2.0 (multiplet overlapping with acetone, -CH_2-), 2.0-1.0 (multiple overlapping signals, -CH_3 groups of backbone and side-chain) (Figure S2).

Synthesis of the viologen-modified redox polymer *co*P(N_3MA^{85}-GMA^{15})-vio: *co*P(N_3MA^{85}-GMA^{15}) (68.5 mg, con. 70 mg/ml in acetone; 87 wt% accounts for N_3MA corresponding to 59.7 mg, 0.35 mmol) was diluted with acetone (8 ml) in a Schlenk tube (dried by three Ar-vacuum cycles). (1-(5-Hexyn-1-yl)-1′-methyl-4,4′-bipyridinium dihexafluorophosphate (1.1 equiv., 210 mg, 0.39 mmol) were dissolved in dry DMSO (2 ml) and added to the polymer solution. The solution was deaerated by purging with Ar and $Cu(MeCN_4)PF_6$ (1.1 equiv., 145 mg, 0.39 mmol) was added. The orange reaction mixture was heated at 50°C overnight. After cooling down to room temperature, the orange suspension was quenched with diethyl ether (~25 ml) and the polymer was separated by centrifugation (4000 rpm, 10 min). The polymer was washed with diethyl ether (2 × 25 ml), water (3 × 10 ml), and diethyl ether again (2 × 25 ml), and the light brown powder was dried in a vacuum at room temperature overnight. For purification, a portion of the powder was dissolved in DMSO and diluted by dropwise addition of 0.1 M KCl in water. The solution was dialyzed against a 0.1 M KCl solution using ultracentrifugation and membrane filters with a molecular weight cut-off of 5 kDa

Research Article
doi.org/10.1002/elsa.202100100
Chemistry Europe
European Chemical Societies Publishing

(Vivaspin Turbo, Sartorius). After each run (6000 rpm, 30 min), the filters were refilled with 0.1 M KCl solution (10–15 times) to ensure a complete exchange of the native counter ions against Cl^-. The washing solution was tested with $Na_2S_2O_4$ for blue color indicating viologen. Finally, the polymer was washed with pure water (3 × 8000 rpm, 45 min) to remove excess KCl. The final light-yellow solution was diluted to 10 mg/ml. ^{1}H-NMR (200 MHz, D_2O) δ/ppm: 9.1 and 8.5 (multiplets, bipyridine), 7.8 (broad, triazole), 4.8 and 4.5 (broad, overlapping, -CH_2- and CH_3), 4.0, 3.5 and 3.0 (broad, overlapping, -CH_2- and epoxide), 2.72 (broad, -CH_2-), 2.3-0.5 (overlapping, multiple signals, Figure S3). Ultraviolet-visible (in DMSO) λ/nm: 266 (λ_{max}), corresponds to the viologen unit[16] (Figure S4). $E^{1/2}$ = –292 mV versus SHE, estimated from CVs performed in 0.1 M phosphate buffer (pH 7.4) of a 1,7-diaminoheptane electrografted GC electrode (ø = 3 mm) that was modified by drop-casting the polymer solution and drying overnight (Figure S1).

4.5 | Electrode modification

Bioanodes were prepared by modifying carbon cloth (MTI, Carbon Foam Sheet, Porous C, 0.454 mm thick, porosity ≈ 31 µm, coated on one side with a Nafion/Teflon-based microporous film (50 µm), carbon content 5 mg cm^{-2}, EQ-bcgdl-1400S-LD) with a diameter of 1.8 cm. First, the electrode surface was electrografted in 15 mM *N-Boc*-ethylenediamine in 0.15 M $TBABF_4$/MeCN by running 5 CV cycles from 0 to 1.4 V at 50 mV/s. Directly after electrografting, the electrodes were submerged in 4 M HCl in dioxane for at least 1 h, then washed with absolute ethanol and water. For the adhesion layer, a defined volume of the high-viologen loading polymer (10 mg/ml) was drop-casted on the electrode surface coating an area with a diameter of approximately 4 mm and dried overnight at 4°C. For the catalytically active layer, a defined volume of the high-viologen loading polymer was mixed with *Dv*MF [NiFe] hydrogenase (0.882 mM) and 2,2′-(ethylenedioxy)bis(ethylamine) (1:37 EDEA : water, 26 mg/ml) and was drop-casted onto the adhesion layer followed by drying overnight at 4°C.

4.6 | Electrochemical measurements

The electrochemical measurements of all enzyme/polymer electrodes were performed in a gas diffusion cell[16] at room temperature. A thermal mass flow controller (GFC17; Aalborg Instruments and Controls) was used to adjust the gas feed (Ar or H_2), which was provided from the back of the working electrode. Cyclic voltammetry and chronoamperometry measurements were performed with a Reference 600 (Gamry Instruments) potentiostat. A three-electrode electrochemical cell with an Ag/AgCl/3 M KCl reference electrode and a Pt wire counter electrode was employed. All potentials are rescaled with respect to the SHE according to E(SHE) = E(Ag/AgCl/3 M KCl) +210 mV. All experiments were conducted in 0.1 M phosphate buffer (pH 7.3). Prior to measuring, the electrolyte was saturated with Ar. The phosphate buffer was continuously purged with Ar throughout the measurements to prevent O_2 from entering the bulk solution. Prior to the performance tests, the enzyme was reactivated at a potential of –0.59 V versus SHE for 5 min. Afterward, the electrodes were characterized with cyclic voltammetry at a scan rate of 10 mV/s. The characterization was performed both under Ar and H_2. Chronoamperometry measurements were performed at E = +0.16 V vs. SHE for 20 min. After 10 min the gas feed was switched from Ar to H_2.

ACKNOWLEDGMENTS

This project has received funding from the European Union's Horizon 2020 research and innovation program under the Marie Skłodowska-Curie MSCA-ITN "ImplantSens" [813006]. James Birrell acknowledges funding from the DFG in the framework of the SPP 3561927 "Iron–Sulfur for Life" (Project BI 2198/1-1). James Birrell and Wolfgang Lubitz acknowledge the continuous financial support by the Max Planck Society.

CONFLICT OF INTEREST

The authors declare no conflict of interest.

DATA AVAILABILITY STATEMENT

Data are available on request from the authors.

REFERENCES

1. W. Lubitz, H. Ogata, O. Rüdiger, E. Reijerse, *Chem. Rev.* **2014**, *114*, 4081.
2. S. Cosnier, A. J. Gross, A. Le Goff, M. Holzinger, *J. Power Sources* **2016**, *325*, 252.
3. I. Mazurenko, X. Wang, A. de Poulpiquet, E. Lojou, *Sustain. Energ. Fuels* **2017**, *1*, 1475.
4. K. A. Vincent, A. Parkin, F. A. Armstrong, *Chem. Rev.* **2007**, *107*, 4366.
5. A. K. Jones, E. Sillery, S. P. J. Albracht, F. A. Armstrong, *Chem. Commun.* **2002**, 866.
6. A. A. Karyakin, S. V. Morozov, O. G. Voronin, N. A. Zorin, E. E. Karyakina, V. N. Fateyev, S. Cosnier, *Angew. Chem. Int. Ed.* **2007**, *46*, 7244.
7. S. D. Varfolomeev, A. I. Yaropolov, I. V. Berezin, M. R. Tarasevich, V. A. Bogdanovskaya, *Bioelectrochem. Bioenerg.* **1977**, *1977*, 314.
8. N. Mano, A. de Poulpiquet, *Chem. Rev.* **2018**, *118*, 2392.
9. L. Xu, F. A. Armstrong, *RSC Adv.* **2015**, *5*, 3649.
10. A. Ruff, F. Conzuelo, W. Schuhmann, *Nat. Catal.* **2020**, *3*, 214.

11. X. Xiao, H.-q. Xia, R. Wu, L. Bai, L. Yan, E. Magner, S. Cosnier, E. Lojou, Z. Zhu, A. Liu, *Chem. Rev.* **2019**, *119*, 9509.
12. S. V. Hexter, F. Grey, T. Happe, V. Climent, F. A. Armstrong, *PNAS* **2012**, *109*, 11516.
13. N. Plumeré, O. Rüdiger, A. A. Oughli, R. Williams, J. Vivekananthan, S. Pöller, W. Schuhmann, W. Lubitz, *Nat. Chem.* **2014**, *6*, 822.
14. A. A. Oughli, F. Conzuelo, M. Winkler, T. Happe, W. Lubitz, W. Schuhmann, O. Rüdiger, N. Plumeré, *Angew. Chem. Int. Ed.* **2015**, *54*, 12329.
15. A. Ruff, J. Szczesny, S. Zacarias, I. A. C. Pereira, N. Plumeré, W. Schuhmann, *ACS Energy Lett*. **2017**, *2*, 964.
16. J. Szczesny, N. Marković, F. Conzuelo, S. Zacarias, I. A. C. Pereira, W. Lubitz, N. Plumeré, W. Schuhmann, A. Ruff, *Nat. Commun.* **2018**, *9*, 4715.
17. A. Ruff, J. Szczesny, M. Vega, S. Zacarias, P. M. Matias, S. Gounel, N. Mano, I. A. C. Pereira, W. Schuhmann, *ChemSusChem* **2020**, *13*, 3627.
18. J. Szczesny, J. A. Birrell, F. Conzuelo, W. Lubitz, A. Ruff, W. Schuhmann, *Angew. Chem. Int. Ed.* **2020**, *59*, 16506.
19. S. Hardt, S. Stapf, D. T. Filmon, J. A. Birrell, O. Rüdiger, V. Fourmond, C. Léger, N. Plumeré, *Nat. Catal.* **2021**, *4*, 251.
20. V. Fourmond, S. Stapf, H. Li, D. Buesen, J. Birrell, O. Rüdiger, W. Lubitz, W. Schuhmann, N. Plumeré, C. Léger, *J. Am. Chem. Soc.* **2015**, *137*, 5494.
21. M. Rasmussen, S. Abdellaoui, S. D. Minteer, *Biosens. Bioelectron.* **2016**, *76*, 91.
22. D. Leech, P. Kavanagh, W. Schuhmann, *Electrochim. Acta* **2012**, *84*, 223.
23. S. C. Barton, J. Gallaway, P. Atanassov, *Chem. Rev.* **2004**, *104*, 4867.
24. A. de Poulpiquet, D. Ranava, K. Monsalve, M.-T. Giudici-Orticoni, E. Lojou, *ChemElectroChem* **2014**, *1*, 1724.
25. K. So, K. Sakai, K. Kano, *Curr. Opin. Electrochem.* **2017**, *5*, 173.
26. A. E. W. Horst, K.-M. Mangold, D. Holtmann, *Biotechnol. Bioeng.* **2016**, *113*, 260.
27. K. So, Y. Kitazumi, O. Shirai, K. Nishikawa, Y. Higuchi, K. Kano, *J. Mater. Chem. A* **2016**, *4*, 8742.
28. T. Nakagawa, H. Mita, H. Kumita, H. Sakai, Y. Tokita, S. Tsujimura, *Electrochem. Commun.* **2013**, *36*, 46.
29. S. Park, J.-W. Lee, B. N. Popov, *Int. J. Hydrog. Energy* **2012**, *37*, 5850.
30. J. Szczesny, A. Ruff, A. R. Oliveira, M. Pita, I. A. C. Pereira, A. L. de Lacey, W. Schuhmann, *ACS Energy Lett.* **2020**, *5*, 321.
31. C. Fichtner, C. Laurich, E. Bothe, W. Lubitz, *Biochem*. **2006**, *45*, 9706.
32. S. Pöller, M. Shao, C. Sygmund, R. Ludwig, W. Schuhmann, *Electrochim. Acta* **2013**, *110*, 152.
33. R. A. S. Luz, A. R. Pereira, J. C. P. de Souza, F. C. P. F. Sales, F. N. Crespilho, *ChemElectroChem* **2014**, *1*, 1751.

SUPPORTING INFORMATION

Additional supporting information may be found in the online version of the article at the publisher's website.

How to cite this article: A. Lielpetere, J. M. Becker, J. Szczesny, F. Conzuelo, A. Ruff, J. Birrell, W. Lubitz, W. Schuhmann. *Electrochem. Sci. Adv*. **2022**, *2,* e2100100. https://doi.org/10.1002/elsa.202100100